Journal of Biomedical Optics

BiomedicalOptics.SPIEDigitalLibrary.org

Optical coherence tomography for blood glucose monitoring *in vitro* through spatial and temporal approaches

Lucas Ramos De Pretto
Tania Mateus Yoshimura
Martha Simões Ribeiro
Anderson Zanardi de Freitas

SPIE.

Lucas Ramos De Pretto, Tania Mateus Yoshimura, Martha Simões Ribeiro, Anderson Zanardi de Freitas, "Optical coherence tomography for blood glucose monitoring *in vitro* through spatial and temporal approaches," *J. Biomed. Opt.* **21**(8), 086007 (2016), doi: 10.1117/1.JBO.21.8.086007.

Optical coherence tomography for blood glucose monitoring *in vitro* through spatial and temporal approaches

Lucas Ramos De Pretto,[a,b] Tania Mateus Yoshimura,[a,b] Martha Simões Ribeiro,[a] and Anderson Zanardi de Freitas[a,*]
[a]Nuclear and Energy Research Institute, Av. Professor Lineu Prestes, 2242, São Paulo, SP, 05508-000, Brazil
[b]University of São Paulo, Postgraduate Program in Nuclear Technology, Av. Professor Lineu Prestes, 2242, São Paulo, SP, 05508-000, Brazil

Abstract. As diabetes causes millions of deaths worldwide every year, new methods for blood glucose monitoring are in demand. Noninvasive approaches may increase patient adherence to treatment while reducing costs, and optical coherence tomography (OCT) may be a feasible alternative to current invasive diagnostics. This study presents two methods for blood sugar monitoring with OCT *in vitro*. The first, based on spatial statistics, exploits changes in the light total attenuation coefficient caused by different concentrations of glucose in the sample using a 930-nm commercial OCT system. The second, based on temporal analysis, calculates differences in the decorrelation time of the speckle pattern in the OCT signal due to blood viscosity variations with the addition of glucose with data acquired by a custom built Swept Source 1325-nm OCT system. Samples consisted of heparinized mouse blood, phosphate buffer saline, and glucose. Additionally, further samples were prepared by diluting mouse blood with isotonic saline solution to verify the effect of higher multiple scattering components on the ability of the methods to differentiate glucose levels. Our results suggest a direct relationship between glucose concentration and both decorrelation rate and attenuation coefficient, with our systems being able to detect changes of 65 mg/dL in glucose concentration.
[DOI: 10.1117/1.JBO.21.8.086007]

Keywords: noninvasive; diabetes; attenuation coefficient; speckle decorrelation; glycemic control; mouse blood.

Paper 160101PRRR received Feb. 19, 2016; accepted for publication Jul. 25, 2016; published online Aug. 16, 2016.

1 Introduction

Every year noncommunicable diseases (NCDs) cause millions of deaths. According to the World Health Organization (WHO),[1] in 2008, for instance, this number reached 36 million, corresponding to 63% of all deaths in that year. Responsible for nearly 50% of all NCDs deaths, cardiovascular diseases (CVDs) and diabetes are preventable in 80% of the cases.[2] The burden associated with those ailments extends beyond the mortality and treatment costs, affecting quality of life and productivity. Brazil, in 2005, lost USD 2.7 billion of national income due to diabetes and CVDs, and this expenditure was expected to triple by 2015, according to WHO.[3] However, the International Diabetes Federation (IDF) reported that the actual expenditure was over USD 21 billion,[4] far surpassing the prediction.

Major risk factors for type 2 diabetes mellitus and CVD, such as dysglycemia, hypertension, atherogenic dyslipidemia, and abdominal obesity, make up a medical condition known as metabolic syndrome (MetS) and are predictors for the development and advance of the aforementioned diseases. Simultaneous occurrence of these risk factors is accompanied by an oxidative stress state and endothelial dysfunction,[5] and the prevalence of high blood glucose levels, as is the case for diabetic and prediabetic patients, largely contributes to this scenario, since glucose, in elevated concentrations, may form covalent links with endothelial proteins and change their function.[6,7]

Continuous monitoring of glucose level is thus of great importance for the prevention and diagnosis of MetS. The most common method for that goal today is the use of portable glucometers.[8] However, as these devices require blood samples collected through skin puncture, a number of obstacles arise for adherence of patients to the treatment, including fear of the needle, pain, and discomfort, among others.[9] Moreover, the use of test strips, as is the case for portable glucometers, increases the total cost of self-monitoring, which is yet another barrier to the approach.[9] As an example, in 2012, this cost was USD 770 per patient in the United States.[10] Ergo, noninvasive methods may increase the effectiveness of self-monitoring of glucose levels while reducing the costs and waste produced during treatment. For that reason, it was not long before many different techniques were adapted to glucose sensing, trying to fill the gap for a noninvasive diagnostic approach. Such techniques include fluorescence sensors,[11] time-of-flight measurements,[12,13] and even nonoptical modalities like amperometric biosensors[14] and impedance spectroscopy.[15]

Optical coherence tomography (OCT) has been widely used in clinical applications,[16] and its ability to assess blood properties *in vitro*[17] and *in vivo*[18] has been demonstrated. Consequently, it is not surprising that adaptations of OCT have been studied to noninvasively monitor glucose. In this work, we further explore OCT as a noninvasive method for the monitoring of glycemia through a simple analysis of optical attenuation. We report our findings on the measured optical

*Address all correspondence to: Anderson Zanardi de Freitas, E-mail: freitas.az@ipen.br

1083-3668/2016/$25.00 © 2016 SPIE

attenuation coefficient (μ) for different blood sugar levels for diluted and undiluted blood samples *in vitro*. Additionally, the effects of varying blood glucose concentrations on the OCT speckle pattern are evaluated through the autocorrelation of the signal. The OCT has been reported to differentiate the viscosity of blood samples,[19,20] and we extend those studies with our method and with different blood sugar concentrations. Both analyses with OCT are performed as preliminary viability studies for the techniques.

2 Methodology

2.1 *Sample Preparation*

Blood samples were drawn through cardiac puncture from C57BL/6 female mice with ages ranging from 6 to 8 weeks, while they were kept under deep anesthesia. All procedures were conducted in accordance with the Guidelines for the Care and Use of Laboratory Animals[21] and were approved by the institutional animal ethics committee. Euthanasia was performed by overdose of chemical anesthetics, and death was confirmed by cervical dislocation.

After blood collection, the samples were heparinized (166 IU/mL) to prevent coagulation and 90 μL aliquots were distributed in triplicate over a 96-well microtiter plate. Four groups were devised by adding glucose solutions with different concentrations. The solutions were prepared with phosphate-buffered saline (1 M, pH 7.4) with increasing concentrations of glucose [D - (+) - Glucose, Sigma-Aldrich] between 160 and 310 mg/dL, with addition steps of 50 mg/dL. Aliquots of 10 μL of these solutions were added to the wells previously filled with heparinized blood, resulting in a final volume of 100 μL per well.

Intending to study the effect of a high multiple scattering component of the signal attenuation, as is the case when probing through biological tissue,[22,23] a second experiment was performed with a new round of blood collection. Aiming to minimize possible errors during preparation, we decided to work with only one glucose solution (530 mg/dL in concentration) for the new samples. By simple dilutions, several glucose concentrations were obtained from this high-concentrate solution. This time, glucose was diluted in an isotonic saline in order to obtain the intended higher multiple scattering effect, as previously described by Popescu et al.[24] These glucose solutions were added to heparinized blood, again placed in a 96-well microtiter plate, and the final samples were composed of 40 μL of heparinized blood and 60 μL saline-glucose solution, totaling a final volume of 100 μL per sample.

For both sets of experiments, the samples were carefully handled and maintained under controlled temperature (18°C) to avoid blood degradation and hemolysis during the experimental course. Before each data collection (blood glucose assessment, OCT measurements, and speckle analysis), each sample was slowly homogenized per the standard with a micropipette in order to prevent sedimentation, as OCT has been shown to be sensitive to effects caused by blood aggregation and sedimentation.[25]

2.2 *Blood Glucose Assessment*

For reference, blood glucose levels were assessed in duplicate by a portable glucometer (OneTouch® Ultra®, Johnson & Johnson Medical Devices & Diagnostics). Strips were positioned directly over the blood samples' surface inside the wells after careful homogenization, and measurements were conducted immediately before and after data acquisition.

2.3 *Optical Coherence Tomography Measurements*

For each blood sample, 100 consecutive acquisitions (B-scans) were performed at the same location with a commercial Spectral Radar OCT system OCP930SR (Thorlabs Inc.) with a central wavelength of 930 nm, spectral bandwidth (FWHM) of 100 nm, and spatial resolution of 6 μm (lateral and axial) in the air. Each B-scan was 2000×512 pixels in size, covering 4 mm of the sample (laterally). Those B-scans were then analyzed via software for calculation of the attenuation coefficient. In order to correct the depth probed in the acquisitions, aliquots of 0.5 μL were collected from every sample and placed on glass slides for determination of the refractive index (RI).

Custom software was developed for the analysis using a simple exponential decay model for the attenuation of the OCT system based on Beer–Lambert's law,[26] as follows:

$$I(z) = I_0.e^{-2\mu z} + C, \tag{1}$$

where $I(z)$ is the intensity at depth z, I_0 is the source intensity, μ is the measured attenuation coefficient in our OCT system, and C is a constant accounting for background noise.

Such an approach, albeit simplistic, is able to differentiate the effect of varying samples on the attenuation of the OCT signal. More robust methods have been described in the literature, and are able to account for system-dependent and multiple-scattering effects, which affect OCT sampling of turbid media.[27] However, as in this viability study, the samples were under a controlled environment and care was taken to avoid time- and temperature-dependent aberrations; the fundamental difference in the aliquots analyzed was the glucose concentration, our parameter of interest. As such, it is the major source of variance in the combined effect of whole blood on OCT signal attenuation. Therefore, the main goal in using the Beer–Lambert's law approach was to perform fast and easy-to-compute analysis of attenuation that would enable the visualization of the overall trend of μ across the samples.

Once a B-scan is loaded in the software, the user selects a region of interest and its A-scans are first aligned through a peak-finding function to compensate for irregularities or displacements of the sample, then averaged. A fitting of the model in Eq. (1) is performed in the resulting A-scan, and parameters I_0, μ, and C are obtained. For the present study, the value of interest is μ. The process is repeated for all 100 B-scans of every sample.

2.4 *Speckles in Optical Coherence Tomography*

Speckles in the OCT arise as a consequence of the sensitivity to the phase of the cross-correlation of the probed and reference optical fields.[28] Nevertheless, the speckle pattern has intensity fluctuations over time, dependent on the behavior of the scatterers inside the sample. This makes it possible to differentiate samples through an analysis of the OCT signal's intensity.

One approach to such an analysis is the autocorrelation of the OCT signal. An area of the sample is probed, acquiring consecutive A-scans. A single point p in the A-scans is studied through time. Its intensity variations will alter the autocorrelation values, which will decay to zero (i.e., no longer correlated) at different rates for different behaviors of the speckle pattern.

For N A-scans acquired consecutively, the normalized autocorrelation for the point p may be written as

$$R(p,\tau) = \frac{\sum_{t=1}^{N-\tau}(I_{p,t} - \langle \mathrm{I} \rangle)(I_{p,t+\tau} - \langle \mathrm{I} \rangle)}{\sum_{t=1}^{N}(I_{p,t} - \langle \mathrm{I} \rangle)^2}, \quad (2)$$

in which $I_{p,t}$ is the intensity of the point p at a given time t, τ is the lag interval, and $\langle \mathrm{I} \rangle$ is the temporal average. Calculating R for varying time lags results in an array of autocorrelation values for increasing intervals. For zero time lag, there is total correlation, and the value should decrease as the intervals increase.

This calculation is repeated for 20 different sets of 1024 consecutive A-scans, and the autocorrelation values are averaged. A new point p is assigned, and another iteration is performed. The range of points evaluated is chosen via user input in custom software, and it determines different depths for analysis. The acquisitions were performed with the beam directed at a small angle (~8 deg) from the normal to the blood surface, to eliminate specular reflections. All the samples were at room temperature.

As fluctuations of intensity occur rapidly in time, a custom OCT system (1325 nm central wavelength) was built, as described elsewhere,[29] achieving an 8-kHz acquisition rate. Also, as demonstrated in our previous work, an observation parameter τ_c is defined as the time interval it takes for the autocorrelation values to decay to $1/e$.[29] This approach is fast, and the value of τ_c is easily obtained and is still sensitive to changes in the temporal behavior of speckles, which makes it interesting for future *in vivo* applications.

This OCT system, however, was not used for total attenuation calculations, as the software developed for its signal acquisition was optimized for temporal analysis, with a lower axial resolution than the OCP930SR. Therefore, all attenuation studies were carried out with a 930-nm OCT.

2.5 *Statistical Analysis*

Glucose measurements are arithmetic means with their respective standard deviations. The average attenuation coefficient is obtained from 100 measurements for every sample and presented as a function of glucose concentration. Attenuation coefficient data were submitted to the Kolmogorov–Smirnov test, which attested they were not to be drawn from a normally distributed population, so multiple mean comparisons were performed using the Kruskal–Wallis test with Dunn's as posttest. Diluted blood was further submitted to K-means cluster analysis to identify groups of similar data.

Speckle decorrelation data are withdrawn from a normal distribution according to the Shapiro–Wilk normality test. Therefore, one-way analysis of variance was performed, followed by Bonferroni's for a multiple comparison test.

All data analyses were performed with GraphPad Prism 5 and OriginPro 9.1 software, and we assumed statistically significant values for $p < 0.05$.

3 Results and Discussion

3.1 *Attenuation Coefficient*

Our results for the obtained glucose concentrations in whole blood for attenuation coefficient analysis are presented in Table 1. The resulting glucose concentrations deviated from our expectations, presumably due to precision limitations of instruments used during sample preparation (dilution and weighing).

Table 1 Whole blood glucose concentrations for each group ($n = 12$). Values are presented as means ± SD.

Groups	Blood glucose (mg/dL)
1	229 ± 09
2	294 ± 06
3	384 ± 11
4	517 ± 31

This first range of blood glucose concentrations displayed good correlation between the computed μ value and the blood sugar levels, as reported in Fig. 1.

Our results show a trend of increase of the signal attenuation with respect to growing glucose levels. Nevertheless, studies in the literature report the use of glucose as an optical clearing agent in biological applications,[30,31] and OCT studies have shown a decrease in attenuation with increasing glucose concentrations.[32] This is a consequence of RI matching between the plasma and the erythrocytes,[33] and is also due to aggregations and changes in size of red blood cells (RBCs), as was suggested by Tuchin et al.[34] However, it was also reported by Tuchin that the total attenuation coefficient of blood increased when mixed with glucose *in vitro*,[34] and related work shows the increase trend up to 10,000 mg/dL[35] *in vitro*. Such a value, nonetheless, lies far outside the normal glucose levels recommended for euglycemic subjects (between 70 and 100 mg/dL according to Standards of Medical Care in Diabetes[36]). These apparently contrasting results, however, have been observed and explained by Bednov et al.[37] in the near-infrared region. The increase in μ with the addition of

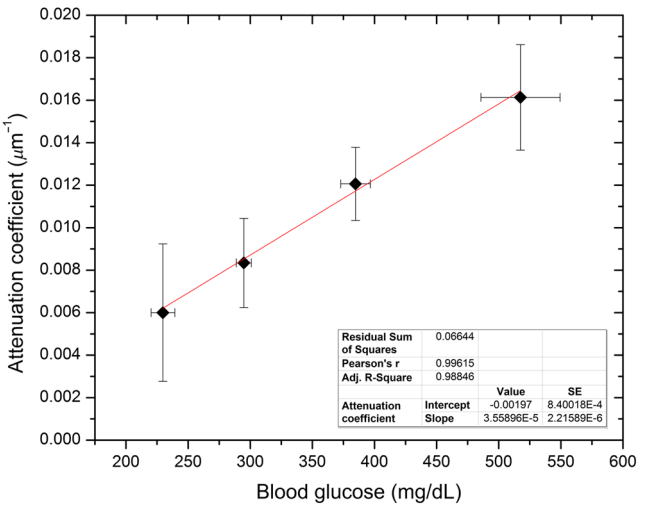

Fig. 1 Attenuation coefficients calculated in relation to average glucose concentrations from whole blood after RI correction (IR = 1.26). Multiple comparison analysis showed $p < 0.001$ between every group (Kruskal–Wallis with Dunn's as post hoc). Red line represents the best linear correlation obtained, with slope of 3.55e-5 mg/dL · μm with an adjusted R^2 of 0.98, which indicates that a linear model is suitable for our data. SE = standard error.

glucose is a direct result of the osmotic shock of RBCs when in the hyperglicemic condition, deforming their normal shape and directly affecting the scattering properties of blood.[38] Such a change in the scattering coefficient greatly surpasses the effects of index matching, raising the total attenuation of the signal, and affects both sedimented and nonsedimented blood. Furthermore, the aforementioned study shows that a higher glucose concentration means a higher osmotic shock effect, which linearly scales up attenuation, matching our observations. Nevertheless, the reported glucose levels tested exceed the physiologic range. Our results, thus, show that the μ increase trend is also true for lower glucose levels closer to normal glucose concentrations. Moreover, it also demonstrates the sensitivity of OCT to the osmotic shock of RBCs. Still, the linear trend observed due to osmotic effects, associated with our glucose levels (all within physiologic scope), explains the absence of the so-called concentration-dependent scattering,[27] which induces a nonlinear relation between scattering and concentration of scatterers in the medium.

However, it has been suggested that time after mixing plays a major role in the optical clearing effect *in vivo*,[31] and that was also confirmed for osmotic shock,[37] which is temporary as the RBCs adapt to the hyperglicemic conditions after ~10 min. All our measurements were performed within 5 min after the addition of glucose, so all were affected by the discussed condition. After the period of adaptation of RBCs, the scattering coefficients normalize, and index matching promotes the results observed in optical clearing studies. Such an observation on the morphology of erythrocytes, then, conciliates both types of results observed in the literature.

Statistical analysis reported significant differences for the attenuation coefficient among all groups with $p < 0.001$ for blood glucose concentrations in the range of 230 to 517 mg/dL. Due to the fact that spacing (in glucose levels) between our groups varies greatly, it is not possible to define a differentiating resolution for the approach, but differences as low as 65 mg/dL (between groups 1 and 2) were detectable.

Despite our samples' concentrations still surpassing the values of normoglycemic subjects, patients with diabetic ketoacidosis were reported to have plasma glucose levels above 250 mg/dL, and severe crises of hyperglycemia crises may reach values exceeding 600 mg/dL,[39] which places our tests within a biologically valid range.

The temporary characteristic of osmotic shock, allied with the fact that such an effect occurs only *in vitro*, is a limiting factor on the proposed technique and greatly hinders its clinical application. Notwithstanding this, the proposed methodology was still followed in the subsequent experiments to fully report on the observation of hyperglicemic shock through OCT.

In our second experiment with diluted blood, we have obtained more data points with different glucose concentrations. However, no linear correlation could be observed with this new set of data, as was the case for whole blood. The dilution of blood in isotonic saline solution to about 40% results in a stronger multiple scattering component in the OCT signal, as proposed by Popescu.[24] Associated with it is the fact that dilution directly affects the glucose concentration needed for the osmotic difference between RBCs and the serum to produce an appreciable change in the attenuation coefficient, which means that smaller additions of glucose will not be detectable by our approach, effectively lowering the resolution for differentiation. To confirm that hypothesis and search for correlations between μ and blood sugar, K-means clustering analysis was performed. The goal was to group together the concentrations with similar attenuation, enabling the observation of the necessary addition of glucose for differences noticeable by the technique. We were able to ascertain that there are three distinct groups in the range of glucose levels tested, as presented in Fig. 2.

If one considers the distance between group centers identified by the K-means, an approximate resolution may be defined as the average of those distances. In the reported case, the distances are 120 mg/dL (cluster 1 to 2) and 146 mg/dL (cluster 2 to 3), giving a resolution of 133 mg/dL for the diluted samples, lower than the one obtained with whole blood. To ease visualization of those results, the average glucose concentration and μ of each group was calculated and plotted as new datapoints as a function of blood sugar levels. This plot is presented in Fig. 3, and the calculated values, along with standard deviation, are in Table 2.

It is now possible to see once more the increasing tendency in the attenuation coefficient, and a linear fitting was performed. The fit reported a slope of 1.34e to 5 mg/dL $\cdot$ μm and an R^2 value of 0.99, suggesting that a linear model is adequate for our data. Furthermore, the clusters were subjected to the Kruskal–Wallis test with Dunn's for multiple mean comparisons, and significant differences were observed between them ($p < 0.05$).

3.2 *Speckle Decorrelation*

The literature suggests that glucose levels directly affect blood viscosity.[40] Furthermore, viscosity of a medium is a determinant factor for the Brownian motion of particles suspended in such a medium, as indicated by the Stokes–Einstein equation for the diffusion coefficient. As the viscosity is inversely proportional to the latter, it is expected to be directly proportional to the decorrelation time of the Brownian motion. Autocorrelation analysis of the OCT signal has been shown to be able to discriminate between different blood viscosities due to salt[19] and glucose in high concentrations.[20] The decorrelation times calculated by our method, therefore, are expected to be greater for the highest glucose concentrations.

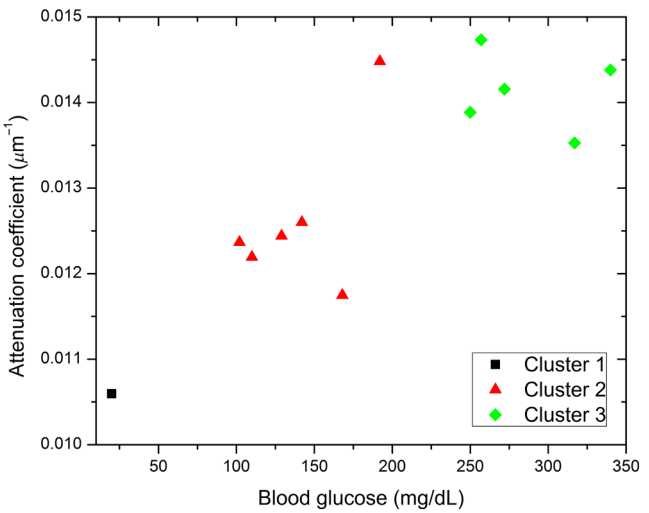

Fig. 2 After RI depth correction (IR = 1.45), attenuation coefficients were calculated in relation to glucose concentrations from diluted blood and grouped in clusters by the K-means method.

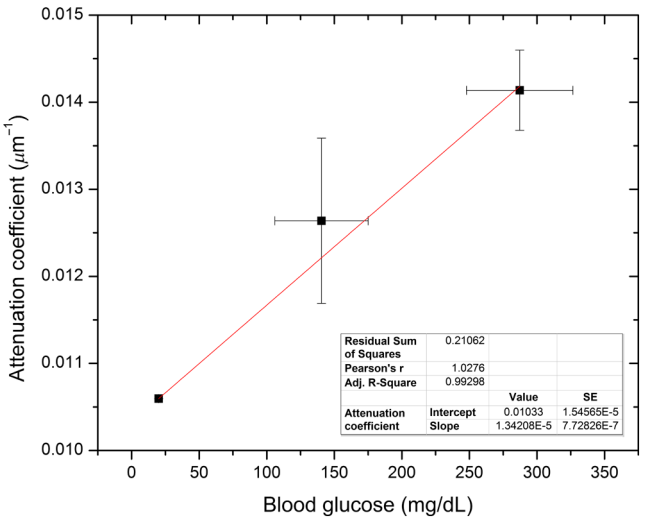

Fig. 3 Mean attenuation coefficients calculated in relation to average glucose concentrations from diluted blood. Multiple comparison analysis showed $p < 0.001$ between every cluster (Kruskal–Wallis with Dunn's as post hoc). Red line represents the best linear correlation obtained, with an adjusted R^2 of 0.99 indicating our data can be represented by a linear model. SE = standard error.

Table 2 New groups resulting from our K-means analysis of diluted blood samples ($n = 12$). Data are presented as mean ± SD.

Groups	Blood glucose (mg/dL)
Cluster 1	20 ± 0
Cluster 2	140 ± 34
Cluster 3	287 ± 34

The concentrations tested in this experiment are presented in Table 3. They were all aliquots from the same blood sample, and the reference glucose values were measured with the portable glucometer, which does not operate for values below 20 mg/dL. Group A did not receive glucose additions. The blood samples used were diluted with isotonic saline, as described previously, to introduce a stronger multiple scattering component to simulate conditions closer to the ones obtained when probing through tissue.

Autocorrelation analysis was performed in regions 18 μm below the first peak of the signal, and each region covered

Table 3 Blood glucose concentrations for each group ($n = 15$). Values are presented as means ± SD.

Groups	Blood glucose (mg/dL)
A	< 20
B	119 ± 0.5
C	220 ± 3
D	300 ± 1
E	354 ± 2

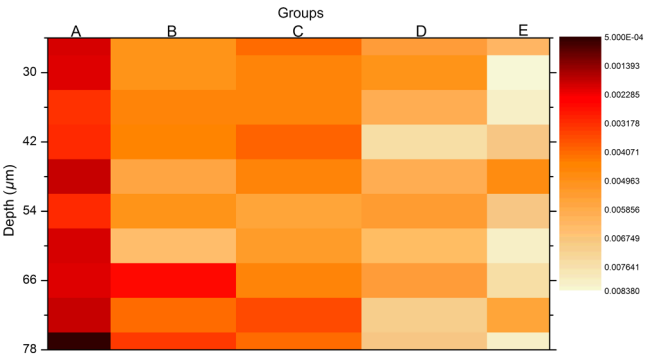

Fig. 4 Decorrelation times presented as a function of depth and blood glucose concentration (different groups) in false color mapping. Darker colors represent shorter times.

60 μm (10 points) in depth. There were intrasample variations in the decorrelation times calculated, which may be due to the rapidly decreasing signal for our system. Nevertheless, there is a clear trend of increase in the decorrelation values, as may be observed in the image plot performed on the matrix with the values, as shown in Fig. 4.

In Fig. 4, darker colors represent shorter decorrelation times, whereas brighter colors represent longer times. It is possible to see in that plot the tendency of the decorrelation times to be greater as the glucose levels get higher. Although each column does present variation in the color, they are still concentrated around certain tones, and such tones are lighter for the rightmost columns. This is a desired result for the technique and follows the expected outcome based on literature reports.

However, to observe only the difference intergroup, one may take the average of all the depths and plot the result as a representative value for each sample. This was done in Fig. 5.

Once more, the direct relationship between the decorrelation rate and glucose concentration is apparent. However, the data for 120 mg/dL require attention. This point does not follow the trend observed for the remaining values and unfavorably affects the linear growth of decorrelation time through sugar levels. It is especially notable in the linear fit (red line) performed.

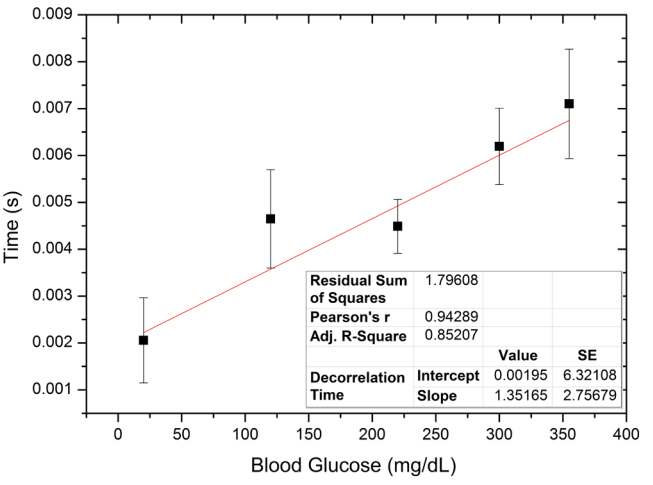

Fig. 5 Average decorrelation times calculated for different blood glucose concentrations. One-way analysis of variance showed $p < 0.05$ between every group (Bonferroni's for multiple comparisons). Red line represents best linear fit.

Even with the error bars, the fit barely crosses this data point. Consequently, the R^2 for this fit is only 0.852, and the residual sum of squares is high. That may indicate that a linear model is not suitable for our data and may not be a good guess. However, as the remaining points do have a good linear fit (R^2 of 0.97), another possibility is the 120 mg/dL sample may have been badly sampled, or each glucose concentration may need more analyzed points for the average to be a good representative. In such a case, the linear trend may be an acceptable model for the observed relation and cannot be disregarded. Further studies will be performed to check each hypothesis.

The obtained results suggest that high glucose levels increase the viscosity of the blood, which is in good agreement with other reports from the literature. The increase in the decorrelation time of speckles in the OCT has been observed before,[20] but the range of concentrations tested lies outside the range of normoglycemic subjects and commonly found glucose levels in diabetic patients.[20,36,39] We aimed to test the ability of OCT to differentiate blood sugar in lower concentrations, with the highest one studied in our trials (~355 mg/dL) coinciding with the lowest already reported (~360 mg/dL or 20 mM). Nevertheless, the approach to the autocorrelation of our study also differs from the one already reported, being based on a parameter readily obtainable from the data, enabling a faster result but still able to discriminate the samples.

Our results thus, along with others works evaluating OCT's signal autocorrelation capacity to detect changes in blood viscosity, indicate OCT as a potential tool for noninvasive diagnostics. Nonetheless, apart from the linear model validation, studies will also be conducted on the technique's resolution for different glucose concentrations, which needs to be improved for a real application. Still, despite being performed *ex vivo*, those results are a base for a noninvasive *in vivo* approach for glucose monitoring with OCT. It has been demonstrated that the time-varying speckles originating from blood are still detectable by OCT *in vivo*,[41] which further supports the possible application of speckle decorrelation analysis.

3.3 *General Considerations*

Our results suggest that the attenuation coefficient is a feasible way to differentiate glucose levels in blood samples using OCT.

Nevertheless, the technique was studied only under osmotic shock conditions, and *in vivo* applications may not be viable, as these effects are only reproducible *in vitro*. Still, such results demonstrate the sensibility of OCT to the shape of RBCs and the consequent change in scattering it promotes on whole blood. Care must thus be taken when using OCT to study glucose-dependent parameters, as time after dilution plays a pivotal role in signal attenuation.

A greater variety of glucose concentrations may reveal the differentiating resolution of the method for whole blood, but with the data from the performed tests, differences of 65 mg/dL were detected. However, in the presence of a greater multiple scattering component, as in the case of saline-diluted blood, this resolution was greatly impacted, and the average resolution was calculated to be 133 mg/dL, half the sensitivity reported for whole blood.

Also, the decorrelation time, defined as a simple parameter in the OCT autocorrelation signal, was shown to be sensitive to different glucose levels in the blood samples, as the addition of glucose alters the viscosity of the medium and therefore the Brownian motion of particles suspended in the plasma. Those distinct behaviors from the particles affect the speckle pattern observed in OCT and are enough to enable differentiation of blood sugar levels. However, *in vivo* studies are still necessary to check if the effects are still visible when under biological tissue. Notwithstanding this, the speckle decorrelation analysis here used is a novel approach for glucose monitoring and presents promising results, but is still at a preliminary stage. The reported findings are hopefully a starting point for further studies to be performed.

Finally, even though OCT systems are currently restricted to clinical and research environments, a trend to make those systems available for domestic use is observed in the literature.[42,43] Therefore, OCT may be used as a self-monitoring device by patients, and having a variety of analysis techniques already developed for this purpose is of great importance for the social impact of the technology.

4 Conclusions

We have presented two approaches to glucose monitoring using OCT. The approaches are based on different effects on the OCT signal, with the total attenuation coefficient being analyzed spatially, while speckle decorrelation is inherently a temporal behavior.

Our results suggest a direct relationship between glucose concentration and both decorrelation rate and attenuation coefficient, with our systems being able to detect changes of 65 mg/dL in blood glucose concentration.

Probably, the attenuation coefficient was affected by deformation of erythrocytes due to osmotic shock in hyperglicemic condition, and the approach used, based on Beer–Lambert's law, may require improvements to be suitable for *in vivo* applications. The speckle decorrelation analysis, on the other hand, presented positive results and, being a novel technique for glucose level differentiation, needs further study to ascertain its viability for *in vivo* scenarios.

Acknowledgments

The authors would like to thank São Paulo Research Foundation-FAPESP (Grant Nos. 2013/09311-9 and 2014/02564-1) and The National Council for Scientific and Technological Development (CNPq)—Brazil (Grant Nos. 449440/2014-1 and grant #309367/2013-1). LR De Pretto would like to thank FAPESP for the scholarship (Grant No. 2013/05492-9). Finally, the authors thank Gesse Eduardo Calvo Nogueira, PhD, for the discussions and useful insights to this study.

References

1. World Health Organization, "Burden: mortality, morbidity and risk factors," in *Global Status Report on Noncommunicable Diseases*, pp. 9–32, WHO Press, Geneva, Switzerland (2010).
2. World Health Organization, *Preventing Chronic Diseases: A Vital Investment*, WHO Press, Geneva, Switzerland (2005).
3. D. Abegunde and A. Stanciole, *An Estimation of the Economic Impact of Chronic Noncommunicable Diseases in Selected Countries*, p. 21, World Health Organization, Geneva, Switzerland (2006).
4. International Diabetes Federation, *IDF Diabetes Atlas*, p. 142, International Diabetes Federation, Brussels, Belgium (2015).
5. R. S. Xu, "Pathogenesis of diabetic cerebral vascular disease complication," *World J. Diabetes* **6**(1), 54–66 (2015).
6. R. Bucala, "Diabetes, aging, and their tissue complications," *J. Clin. Invest.* **124**(5), 1887–1888 (2014).

7. H. Vlassara and J. Uribarri, "Advanced glycation end products (AGE) and diabetes: cause, effect, or both?," *Curr. Diabetes Rep.* **14**(1), 453 (2014).
8. S. K. Vashist, "Continuous glucose monitoring systems: a review," *Diagnostics* **3**(4), 385–412 (2013).
9. W. M. Ong, S. S. Chua, and C. J. Ng, "Barriers and facilitators to self-monitoring of blood glucose in people with type 2 diabetes using insulin: a qualitative study," *Patient Prefer Adherence* **8**, 237–246 (2014).
10. J. Yeaw et al., "Cost of self-monitoring of blood glucose in the United States among patients on an insulin regimen for diabetes," *J. Manage. Care Pharm.* **18**(1), 21–32 (2012).
11. J. C. Pickup et al., "Fluorescence-based glucose sensors," *Biosens. Bioelectron.* **20**(12), 2555–2565 (2005).
12. M. T. Kinnunen et al., "Measurements of glucose content in scattering media with time-of-flight technique: comparison with Monte Carlo simulations," *Proc. SPIE* **5474**, 11 (2004).
13. A. P. Popov, A. V. Priezzhev, and R. Myllylä, "Effect of glucose concentration in a model light-scattering suspension on propagation of ultrashort laser pulses," *Quantum Electron.* **35**(11), 1075–1078 (2005).
14. R. Badugu, J. R. Lakowicz, and C. D. Geddes, "A glucose sensing contact lens: a non-invasive technique for continuous physiological glucose monitoring," *J. Fluoresc.* **13**(5), 371–374 (2003).
15. A. Caduff et al., "First human experiments with a novel non-invasive, non-optical continuous glucose monitoring system," *Biosens. Bioelectron.* **19**(3), 209–217 (2003).
16. A. M. Zysk et al., "Optical coherence tomography: a review of clinical development from bench to bedside," *J. Biomed. Opt.* **12**(5), 051403 (2007).
17. D. J. Faber et al., "Oxygen saturation-dependent absorption and scattering of blood," *Phys. Rev. Lett.* **93**(2), 4 (2004).
18. S. Y. Chen, J. Yi, and H. F. Zhang, "Measuring oxygen saturation in retinal and choroidal circulations in rats using visible light optical coherence tomography angiography," *Biomed. Opt. Express* **6**(8), 2840–2853 (2015).
19. H. Ullah et al., "M-mode swept source optical coherence tomography for quantification of salt concentration in blood: an in vitro study," *Laser Phys.* **22**(5), 1002–1010 (2012).
20. H. Ullah et al., "Can temporal analysis of optical coherence tomography statistics report on dextrorotatory-glucose levels in blood?," *Laser Phys.* **21**(11), 1962–1971 (2011).
21. N. R. Council, *Guide for the Care and Use of Laboratory Animals*, 8th ed., National Academies Press, United States (2011).
22. J. M. Schmitt, "Optical coherence tomography (OCT): a review," *IEEE J. Sel. Top. Quantum Electron.* **5**(4), 1205–1215 (1999).
23. R. K. Wang, "Signal degradation by multiple scattering in optical coherence tomography of dense tissue: a Monte Carlo study towards optical clearing of biotissues," *Phys. Med. Biol.* **47**(13), 19 (2002).
24. D. P. Popescu et al., "Propagation properties of 1300-nm light in blood-saline mixtures determined through optical coherence tomography," *Proc. SPIE* **6864**, 686408 (2008).
25. V. V. Tuchin, X. Xu, and R. K. Wang, "Dynamic optical coherence tomography in studies of optical clearing, sedimentation, and aggregation of immersed blood," *Appl. Opt.* **41**(1), 258–271 (2002).
26. D. P. Popescu et al., "Assessment of early demineralization in teeth using the signal attenuation in optical coherence tomography images," *J. Biomed. Opt.* **13**(5), 054053 (2008).
27. M. Almasian et al., "Validation of quantitative attenuation and backscattering coefficient measurements by optical coherence tomography in the concentration-dependent and multiple scattering regime," *J. Biomed. Opt.* **20**(12), 121314 (2015).
28. J. M. Schmitt, S. H. Xiang, and K. M. Yung, "Speckle in optical coherence tomography," *J. Biomed. Opt.* **4**(1), 95–105 (1999).
29. L. R. De Pretto, G. E. C. Nogueira, and A. Z. Freitas, "Microfluidic volumetric flow determination using optical coherence tomography speckle: an autocorrelation approach," *J. Appl. Phys.* **119**, 163105 (2016).
30. E. I. Galanzha et al., "Effects of different doses of glucose on scattering properties of skin," *Proc. SPIE* **4707**, 244–247 (2002).
31. R. K. Wang and V. V. Tuchin, "Enhance light penetration in tissue for high-resolution optical imaging techniques by the use of biocompatible chemical agents," *Proc. SPIE* **4956**, 314–319 (2003).
32. A. Popov et al., "Glucose sensing in flowing blood and Intralipid by laser pulse time-of-flight and optical coherence tomography techniques," *IEEE J. Sel. Top. Quantum Electron.* **18**(4), 1335–1342 (2012).
33. M. Brezinski et al., "Index matching to improve optical coherence tomography imaging through blood," *Circulation* **103**, 1999–2003 (2001).
34. V. V. Tuchin, X. Q. Xu, and R. K. Wang, "Sedimentation of immersed blood studied by OCT," *Proc. SPIE* **4241**, 357–369 (2001).
35. O. S. Zhernovaya et al., "Study of optical clearing of blood by immersion method," *Proc. SPIE* **7898**, 78981B (2011).
36. American Diabetes Association, "Standards of medical care in diabetes-2015: summary of revisions," *Diabetes Care* **38**, S4 (2015).
37. A. A. Bednov et al., "Monitoring glucose in vivo by measuring laser-induced acoustic profiles," *Proc. SPIE* **3916**, 9–18 (2000).
38. M. Kinnunen et al., "Effect of the size and shape of a red blood cell on elastic light scattering properties at the single-cell level," *Biomed. Opt. Express* **2**(7), 1803–1814 (2011).
39. A. E. Kitabchi et al., "Hyperglycemic crises in adult patients with diabetes," *Diabetes Care* **32**(7), 1335–1343 (2009).
40. C. Irace et al., "Blood viscosity in subjects with normoglycemia and prediabetes," *Diabetes Care* **37**(2), 488–492 (2014).
41. A. Mariampillai et al., "Speckle variance detection of microvasculature using swept-source optical coherence tomography," *Opt. Lett.* **33**(13), 1530–1532 (2008).
42. S. Tomczewski and L. Salbut, "Mobile optical coherence tomography (OCT) system with dynamic focusing and smart-pixel camera," in *Mechatronics: Recent Technological and Scientific Advances*, R. Jabloński and T. Březina, Eds., pp. 785–791, Springer Berlin Heidelberg, Berlin, Germany (2012).
43. M. S. Hrebesh, "Smartphone based multiple reference optical coherence tomography (MRO™) system," *Biomed. Opt.* BT3A.72 (2014).

Biographies for the authors are not available.